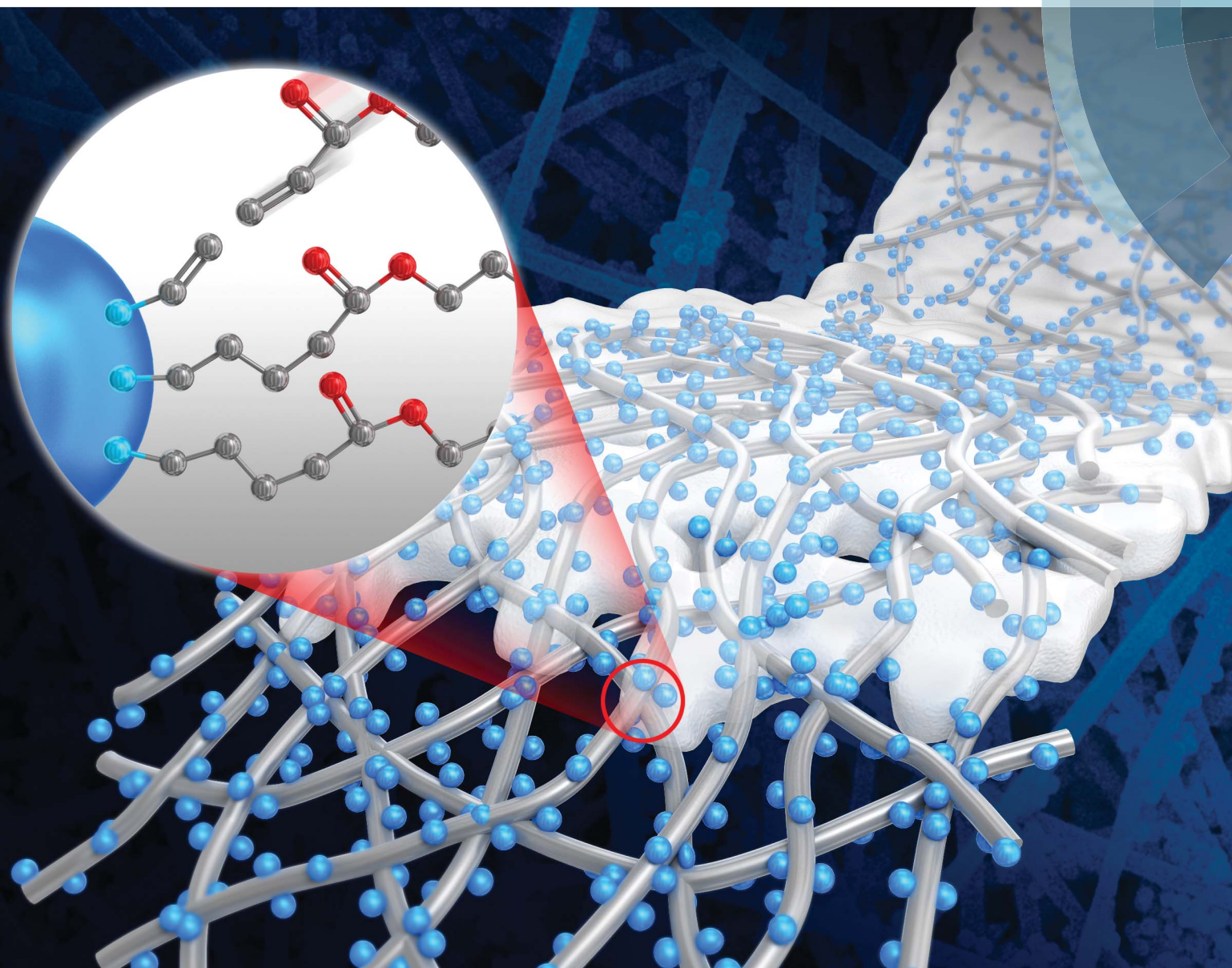


Journal of Materials Chemistry A

Materials for energy and sustainability

www.rsc.org/MaterialsA



ISSN 2050-7488



PAPER

Dong-Won Kim *et al.*

Cycling performance of lithium-ion polymer cells assembled with a cross-linked composite polymer electrolyte using a fibrous polyacrylonitrile membrane and vinyl-functionalized SiO₂ nanoparticles

PAPER

CrossMark
click for updatesCite this: *J. Mater. Chem. A*, 2015, 3, 12163

Cycling performance of lithium-ion polymer cells assembled with a cross-linked composite polymer electrolyte using a fibrous polyacrylonitrile membrane and vinyl-functionalized SiO₂ nanoparticles

Won-Kyung Shin,^a Ji Hyun Yoo,^a Wonchang Choi,^b Kyung Yoon Chung,^b Seung Soon Jang^c and Dong-Won Kim^{*a}

Vinyl-functionalized SiO₂ nanoparticles were synthesized and uniformly dispersed on the surface of a fibrous polyacrylonitrile (PAN) membrane for use as cross-linking sites. A composite polymer electrolyte was prepared by *in situ* cross-linking between vinyl-functionalized SiO₂ particles on the PAN membrane and the electrolyte precursor containing tri(ethylene glycol) diacrylate. The cross-linked composite polymer electrolyte effectively encapsulated the electrolyte solution without leakage. It exhibited good thermal stability as well as favorable interfacial characteristics toward electrodes. Lithium-ion polymer cells composed of a graphite negative electrode and a LiNi_{0.8}Co_{0.15}Al_{0.05}O₂ positive electrode were assembled with the *in situ* cross-linked composite polymer electrolyte. The cells with cross-linked composite polymer electrolytes using the fibrous PAN membrane and vinyl-functionalized SiO₂ particles exhibited high discharge capacity and good capacity retention at both ambient temperature and elevated temperature.

Received 24th February 2015
Accepted 11th March 2015

DOI: 10.1039/c5ta01436k

www.rsc.org/MaterialsA

Introduction

The rapidly expanding use of rechargeable lithium-ion batteries (LIBs) as power sources for portable electronic devices and electric vehicles has led to intensive research on electrolyte systems with favorable electrochemical properties.^{1–5} Traditionally, a mixture of carbonate-based organic solvents that dissolve lithium salts (mostly LiPF₆) is used as the electrolyte material in commercialized LIBs. The liquid electrolyte is characterized by high ionic conductivity, good electrochemical stability and acceptable cycling performance. However, the high flammability of organic solvents in the liquid electrolyte can lead to fire and explosions when short circuit or local overheating accidentally occurs. Therefore, there is a pressing need for safer and more reliable electrolyte systems. Among various electrolyte systems used in rechargeable lithium batteries, the gel polymer electrolyte is a promising candidate due to its high ionic conductivity, film formability and effective encapsulation

of organic solvents in the cell, resulting in the suppression of solvent leakage and enhanced safety.^{6–8} However, polymer hosts in the gel polymer electrolyte usually lose their mechanical strength when they are plasticized by organic solvents. An *in situ* chemical cross-linking method with cross-linking agents has been used to overcome this problem.^{9–16} In this process, an electrolyte solution containing cross-linking agents is injected directly into the cell, and cross-linking is carried out by free radical polymerization triggered by thermal initiation. The obtained gel polymer electrolytes, consisting of a cross-linked polymer network swelled with the liquid electrolyte, have relatively high ionic conductivity and favorable mechanical properties. It has also been reported that the electrochemical properties and mechanical strength of gel polymer electrolytes could be improved with the addition of inert inorganic fillers such as SiO₂, Al₂O₃, TiO₂ and BaTiO₃.^{17–23} In previous studies, we synthesized reactive SiO₂ particles with C=C double bonds on their surface, which permitted the surface reaction with vinyl monomers by free radical polymerization.^{24–27} Encouraged by previous studies, *in situ* cross-linking using these vinyl-functionalized SiO₂ particles is of great interest, because the mechanical properties of gel polymer electrolytes and the electrode–electrolyte interfacial contacts can be enhanced by the combined effect of incorporation of ceramic particles with high mechanical strength and thermal cross-linking induced by reactive SiO₂ particles.

^aDepartment of Chemical Engineering, Hanyang University, Seoul 133-791, Republic of Korea. E-mail: dongwonkim@hanyang.ac.kr; Fax: +82 2 2298 4101; Tel: +82 2 2220 2337

^bCenter for Energy Convergence, Korea Institute of Science and Technology, Seoul 136-791, Republic of Korea

^cSchool of Materials Science and Engineering, Georgia Institute of Technology, Atlanta, GA 30332-0245, USA

In this study, SiO₂ nanoparticles with reactive vinyl groups were synthesized and uniformly dispersed on the surface of a fibrous polyacrylonitrile (PAN) membrane. An *in situ* thermal cross-linking reaction was then induced in the electrolyte solution containing a small amount of tri(ethylene glycol) diacrylate (TEGDA) to form the cross-linked composite polymer electrolyte, as schematically demonstrated in Fig. 1. The cross-linked composite polymer electrolyte was utilized in lithium-ion polymer cells composed of a graphite negative electrode and a LiNi_{0.8}Co_{0.15}Al_{0.05}O₂ positive electrode. The cycling performance of cells was evaluated and compared with those of cells assembled with other PAN-based polymer electrolytes.

Experimental

Synthesis of vinyl-functionalized SiO₂ nanoparticles

SiO₂ nanoparticles with reactive vinyl groups were synthesized by the sol-gel reaction of vinyltrimethoxysilane (VTMS) in aqueous solution, as reported earlier.^{24–27} Briefly, 2 ml of VTMS (Evonik) was added to 150 ml of double-distilled water, and the mixture was stirred until VTMS droplets completely disappeared. Next, 10 ml of an NH₄OH solution (28 wt%, Junsei) was added to the solution and the sol-gel reaction (hydrolysis and condensation) was allowed to proceed for 4 h at 70 °C. After reaction completion, the resulting precipitate was centrifuged and washed several times with ethanol. SiO₂ nanoparticles were obtained as a white powder after vacuum drying at 110 °C for 12 h.

Preparation of the fibrous PAN membrane with reactive SiO₂ nanoparticles

The fibrous PAN membrane was prepared by an electrospinning method, as previously reported.²⁸ PAN (*M_w* = 150 000, Sigma-Aldrich) was dissolved in anhydrous *N,N*-dimethylformamide at 60 °C to a concentration of 10 wt%, and the resulting polymer solution was fed through a capillary tip using a plastic syringe. During electrospinning, a high voltage of 11 kV was applied to

the needle, and the flow rate of the spinning solution was controlled at 0.8 ml h⁻¹. The distance between the tip and the rotating drum collector was 16 cm, and the metal drum was rotated at 200 rpm. Electrospun PAN fibers were collected on aluminum foil wrapped on the drum, and were dried overnight in a vacuum oven at 80 °C before further use. The thickness of the fibrous PAN membrane was controlled at about 35 μm. The coating solution was prepared by dispersing 5 wt% of the vinyl-functionalized SiO₂ nanoparticles in ethanol by sonication for 1 h. The fibrous PAN membrane was then soaked in the coating solution, and the resulting membrane was dried at 70 °C for 24 h.

Electrode preparation and cell assembly

The positive electrode slurry was prepared by mixing 85 wt% LiNi_{0.8}Co_{0.15}Al_{0.05}O₂ (Ecopro Co. Ltd), 7.5 wt% poly(vinylidene fluoride) (PVdF) and 7.5 wt% Super-P carbon (MMM Co.) using *N*-methyl pyrrolidine (NMP) solvent. The slurry was coated onto aluminum foil using a doctor blade. The electrode was dried under vacuum at 110 °C for 12 h. Its active mass loading corresponded to an areal capacity of about 2.0 mA h cm⁻². The negative electrode was prepared similarly by coating an NMP-based slurry of mesocarbon microbeads (MCMB, Osaka Gas), PVdF, and super-P carbon at a weight ratio of 85/7.5/7.5 onto copper foil. To make a gel electrolyte precursor solution, 3.5 wt% of TEGDA (Sigma-Aldrich) was added to the liquid electrolyte with azobisisobutyronitrile (Sigma-Aldrich, 1 wt% of TEGDA) as a thermal radical initiator. A liquid electrolyte consisting of 1.15 M LiPF₆ in ethylene carbonate (EC)/ethylmethyl carbonate (EMC)/diethyl carbonate (DEC) (3 : 5 : 2 by volume, battery grade) containing 5 wt% fluoroethylene carbonate (FEC) was kindly supplied by PANAX ETEC Co., Ltd and used without further treatment. Karl Fisher titration using a Mettler-Toledo Coulometer determined the water content in the liquid electrolyte to be less than 20 ppm. A lithium-ion polymer cell was assembled by sandwiching the fibrous PAN membrane (with and without vinyl-functionalized SiO₂ particles) between the

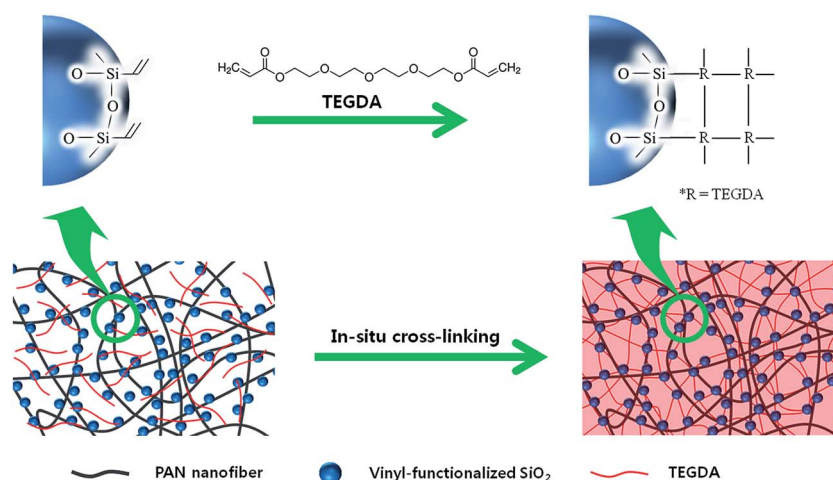


Fig. 1 Schematic illustration of the synthesis of the cross-linked composite polymer electrolyte using the fibrous PAN membrane, vinyl-functionalized SiO₂ nanoparticles and TEGDA.

graphite negative electrode and the $\text{LiNi}_{0.8}\text{Co}_{0.15}\text{Al}_{0.05}\text{O}_2$ positive electrode. The cell was enclosed in a pouch bag injected with the gel electrolyte precursor and was then vacuum-sealed. After assembly, the cells were stored at 70°C for 1 h to induce *in situ* chemical cross-linking. For comparison, a lithium-ion polymer cell was also assembled with a fibrous PAN membrane and the same liquid electrolyte (1.15 M $\text{LiPF}_6\text{-EC/EMC/DEC}$ + 5 wt% FEC) without the cross-linking reaction. Cell assembly was carried out in a dry box filled with argon gas.

Measurements

The morphologies of vinyl-functionalized SiO_2 nanoparticles and fibrous PAN membranes were examined using a field emission scanning electron microscope (FE-SEM, JEOL JSM-6330F). Fourier transform infrared (FT-IR) spectra were recorded on a Magna IR 760 spectrometer with KBr powder-pressed pellets. The thermal shrinking behavior of the polyethylene separator (ND 420, Asahi) and fibrous PAN membranes was examined after being maintained at 150°C for 1 h. The mechanical properties of the PAN-based polymer membranes were measured using a universal test machine (Instron 5966) in accordance with the ASTM D882 method. To measure ionic conductivity and interfacial resistances, AC impedance measurements were performed using a Zahner Elektrik IM6 impedance analyzer over a frequency range of 100 kHz to 1 mHz and amplitude of 10 mV at 25°C . Charge and discharge cycling tests of the lithium-ion polymer cells were conducted at a constant current density of 1.0 mA cm^{-2} (0.5 C rate) over a voltage range of 2.6–4.3 V using a battery cycler (WBCS 3000, Wonatech) at 25 and 55°C , respectively. The HF content in different electrolytes was measured by an acid–base titration method after the cell was stored at 55°C in an oven for 1 week. Methyl orange (Sigma-Aldrich) was used as an acid–base indicator.

Results and discussion

Fig. 2(a) shows the FE-SEM image of vinyl-functionalized SiO_2 nanoparticles obtained by the sol–gel reaction of VTMS. The silica particles had uniform spherical shapes with an average diameter of 250 nm. The FE-SEM images of electrospun PAN membranes without and with reactive SiO_2 nanoparticles are presented in Fig. 2(b) and (c), respectively. The electrospun PAN membrane exhibited a highly porous and interconnected three-dimensional fibrous network structure. This configuration enables absorption of a large amount of electrolyte solution in the porous membrane. As shown in Fig. 2(c), vinyl-functionalized SiO_2 nanoparticles are well distributed in the PAN membrane to provide cross-linking sites throughout the porous membrane. Since SiO_2 particles contain many reactive vinyl groups on their surfaces, they would participate in radical polymerization with TEGDA during *in situ* cross-linking. The gel polymer electrolyte can fully cover the fibrous PAN membrane with SiO_2 particles, which prevents silica particles from detaching from the fibers.

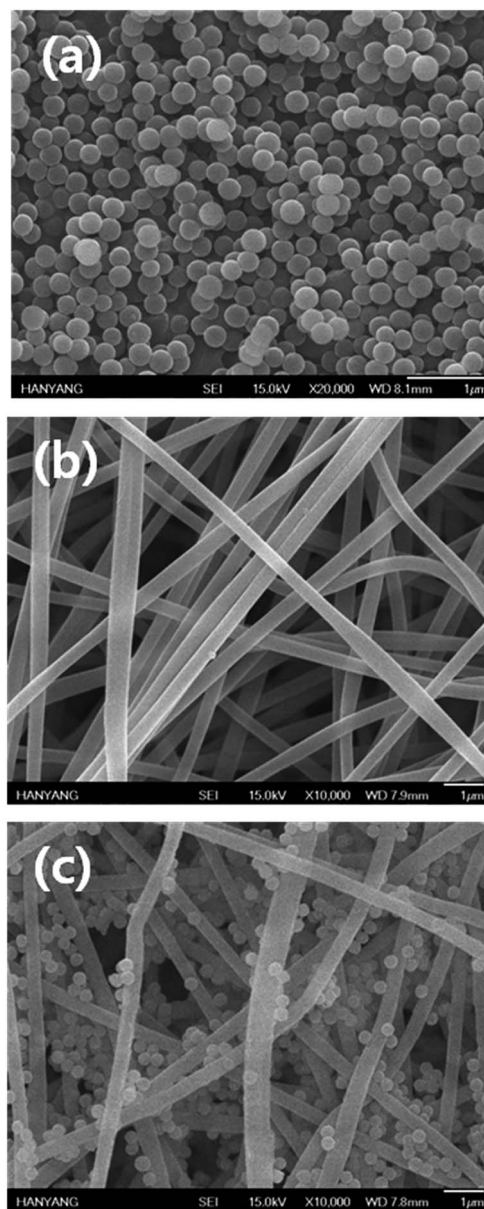


Fig. 2 FE-SEM images of (a) vinyl-functionalized SiO_2 nanoparticles, (b) fibrous PAN membrane, and (c) fibrous PAN membrane with vinyl-functionalized SiO_2 nanoparticles.

The thermal stability of a separator is an important property that affects the safety of lithium batteries at high temperature operating conditions. The polyethylene separator and fibrous composite PAN membranes were stored at 150°C for 1 h to evaluate their heat-resistant properties, and the results are shown in Fig. 3. The polyethylene separator exhibited a high degree of shrinkage during exposure to high temperature conditions. In contrast, fibrous PAN membranes with SiO_2 particles did not show any thermal shrinkage when exposed to the same conditions. This result is attributed to the higher thermal stability of PAN compared to polyethylene and the incorporation of thermally resistant SiO_2 particles into the membrane. The mechanical properties of the PAN-based

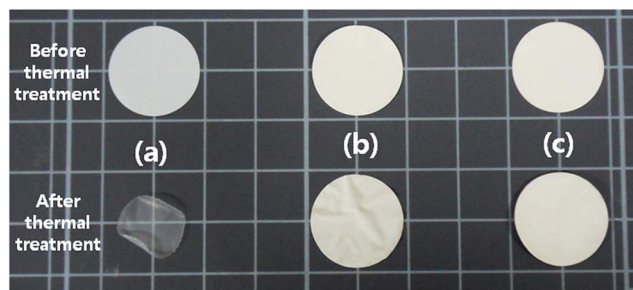


Fig. 3 Photographs of (a) the polyethylene separator, (b) fibrous PAN membrane, and (c) fibrous PAN membrane with vinyl-functionalized SiO₂ particles before and after exposure at 150 °C for 1 h.

polymer membranes were evaluated, and the results are shown in Fig. 4. It is clearly seen that cross-linking using TEGDA in the PAN membranes improved their tensile strength due to the formation of three-dimensional networks. It is noticeable that the incorporation of SiO₂ particles into the PAN membrane greatly improved the tensile strength after the cross-linking reaction. This result implies that the vinyl-functionalized SiO₂ particles with high mechanical strength participate in the chemical cross-linking reaction with TEGDA as cross-linking sites, thereby resulting in the increase of the degree of cross-linking and mechanical properties.

FT-IR analysis was carried out to confirm the chemical cross-linking reaction between vinyl-functionalized SiO₂ particles and TEGDA. The resulting FT-IR spectra are shown in Fig. 5. As depicted in Fig. 5(a), SiO₂ particles showed a characteristic broad band associated with the asymmetric stretching vibrations of Si–O–Si around 1100 cm⁻¹. The presence of C=C double bonds introduced by covalently bonded VTMS molecules in the SiO₂ particles was confirmed by two peaks at 1409 and 1600 cm⁻¹. These peaks are characteristic of C=C double bonds,^{29,30} indicating that the silica particles contained vinyl groups. These vinyl groups permitted further reaction of silica particles with TEGDA to produce the cross-linked composite polymer electrolyte. The peaks observed at 2242 and 1453 cm⁻¹ for the fibrous PAN membrane (Fig. 5(b)) were assigned to the

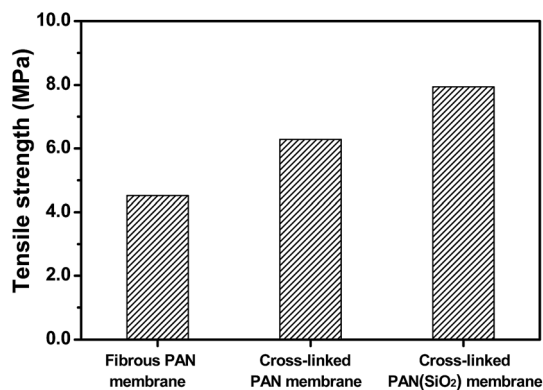


Fig. 4 Tensile strength of PAN-based polymer membranes before and after cross-linking.

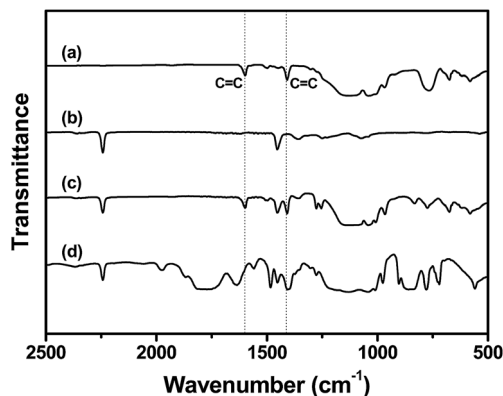


Fig. 5 FT-IR spectra of (a) vinyl-functionalized SiO₂ particles, (b) fibrous PAN membrane, (c) fibrous PAN membrane with vinyl-functionalized SiO₂ particles (before cross-linking), and (d) cross-linked composite polymer electrolyte synthesized from the fibrous PAN membrane, vinyl-functionalized SiO₂ particles and the gel electrolyte precursor containing TEGDA.

C–N stretching vibration and C–H bending vibration, respectively.³¹ The FT-IR spectrum of the cross-linked composite polymer electrolyte presented in Fig. 5(d) revealed that the peaks corresponding to C=C double bonds in the SiO₂ particles disappeared. This result suggests that vinyl groups on the surface of SiO₂ particles react with TEGDA to form the cross-linked polymer electrolyte on the fibrous PAN membrane through free radical polymerization.

Fig. 6(a) presents the FE-SEM image of the cross-linked composite polymer electrolyte synthesized from the fibrous PAN membrane, vinyl-functionalized SiO₂ particles and gel electrolyte precursor. As shown in the figure, the composite PAN membrane containing SiO₂ particles was fully covered with a cross-linked polymer layer containing the electrolyte solution. The composite polymer layer was formed by cross-linking between vinyl-functionalized SiO₂ particles in the fibrous PAN membrane and TEGDA in the gel electrolyte precursor, as schematically illustrated in Fig. 1. Consequently, SiO₂ particles were attached well to PAN fibers through the chemical cross-linking reaction. Moreover, the electrolyte solution was well encapsulated in the cross-linked composite polymer electrolyte without leakage of organic solvents. The silicon EDX mapping image of the cross-linked composite polymer electrolyte shown in Fig. 6(b) illustrates that silica nanoparticles were well dispersed in the composite polymer electrolyte. Thus, the mechanical stability of the cross-linked composite polymer electrolyte was greatly enhanced by the combined effect of uniformly distributed SiO₂ particles and the cross-linked network structure induced by vinyl-functionalized SiO₂ particles.

The *in situ* cross-linked composite polymer electrolyte synthesized with PAN, vinyl-functionalized SiO₂ particles and gel electrolyte precursor was applied to a lithium-ion cell composed of a graphite negative electrode and a LiNi_{0.8}Co_{0.15}Al_{0.05}O₂ positive electrode. The assembled cell was initially subjected to a preconditioning cycle over a voltage range of

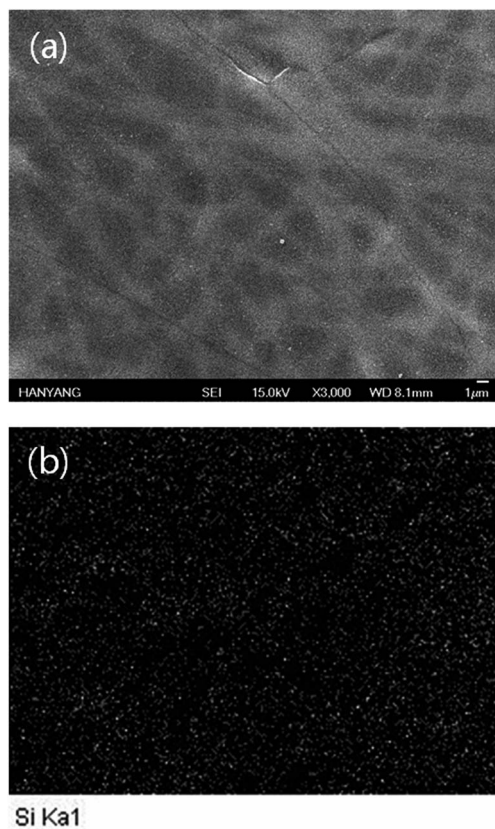


Fig. 6 (a) FE-SEM image and (b) silicon EDX mapping image of the cross-linked composite polymer electrolyte synthesized from the fibrous PAN membrane, vinyl-functionalized SiO₂ nanoparticles and gel electrolyte precursor.

2.6–4.3 V at a rate of 0.1 C. After two cycles at the rate of 0.1 C, the cells were charged at 0.5 C up to a set voltage of 4.3 V. This was followed by constant voltage charge until the final current reached 10% of the charging current. Cells were then discharged down to a cut-off voltage of 2.6 V at the same current rate (0.5 C). Fig. 7(a) shows typical voltage profiles of lithium-ion polymer cells assembled with the PAN(SiO₂)-based cross-linked composite polymer electrolyte. The cell initially delivered a high discharge capacity of 200.4 mA h g⁻¹ based on the active LiNi_{0.8}Co_{0.15}Al_{0.05}O₂ material in the positive electrode. The cell exhibited stable cycling characteristics. It delivered a discharge capacity of 190.0 mA h g⁻¹ after 200 cycles, corresponding to 94.8% of the initial discharge capacity. The cycling results of cells assembled with the liquid electrolyte using a fibrous PAN membrane or the PAN-based cross-linked polymer electrolyte without SiO₂ particles are also given in Fig. 7(b) for comparison. The initial discharge capacity was highest in the cell assembled with the liquid electrolyte using the fibrous PAN membrane. This result is because the cross-linking reaction increases the resistance for ion migration in both the electrolyte and electrodes, reducing the discharge capacity. The ionic conductivities of the liquid electrolyte using the fibrous PAN membrane, cross-linked polymer electrolyte without SiO₂ particles, and cross-linked composite polymer electrolyte with SiO₂ particles

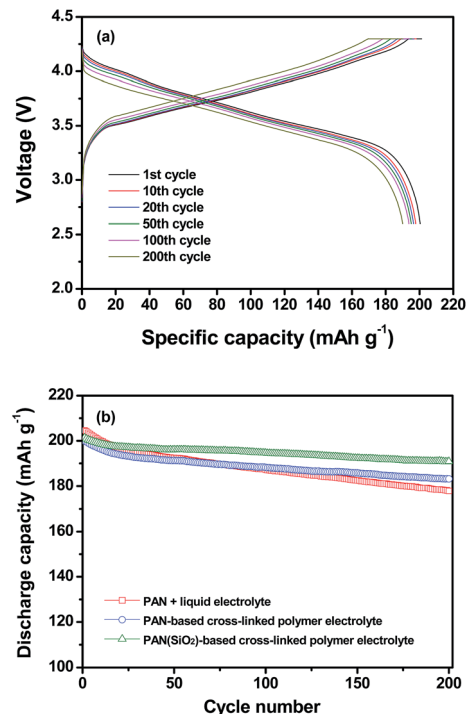


Fig. 7 (a) Charge and discharge curves of a lithium-ion polymer cell assembled with the PAN(SiO₂)-based cross-linked composite polymer electrolyte, and (b) discharge capacities of lithium-ion polymer cells assembled with different polymer electrolytes (0.5 C CC and CV charge, 0.5 C CC discharge, cut-off voltage: 2.6–4.3 V).

were 1.7×10^{-3} , 0.9×10^{-3} , and 1.1×10^{-3} S cm⁻¹, respectively. With respect to cycling stability, cells with the cross-linked polymer electrolyte using PAN or PAN(SiO₂) showed improved capacity retention. After gelling the liquid electrolyte by thermal curing with cross-linking agents (TEGDA and reactive SiO₂ particles), it can serve as an adhesive to bond the PAN membrane and electrodes together, resulting in good capacity retention. As explained above, the ability to retain the electrolyte solution in the cell was greatly enhanced by cross-linking of the liquid electrolyte in the presence of SiO₂ particles, which helped to prevent exudation of the electrolyte solution during cycling.

To understand the cycling behavior of lithium-ion polymer cells with different polymer electrolytes, AC impedance spectra were collected for each type of cell before and after 200 cycles (Fig. 8). All spectra exhibited two overlapping semicircles due to different interfacial resistance contributions. The first semicircle in the higher frequency range is attributed to the resistance due to Li⁺ ion migration through the surface film on electrodes (R_f), and the second semicircle in the middle to low frequency range arises from the charge transfer resistance at the electrode–electrolyte interface (R_{ct}).^{32–34} These AC impedance spectra could be analyzed by using the equivalent circuit given in the inset of Fig. 8(b). In this circuit, R_e is the electrolyte resistance and corresponds to the high frequency intercept at the real axis. R_f and R_{ct} are the resistance of Li⁺ ions through SEI film and the charge transfer resistance, respectively. CPE_i (constant phase element) denotes the capacitance of each

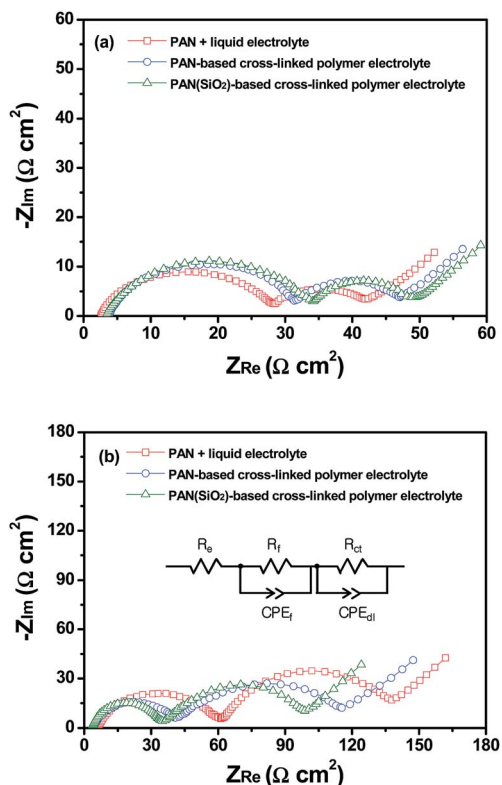


Fig. 8 AC impedance spectra of lithium-ion polymer cells assembled with different polymer electrolytes, which were measured (a) after pre-conditioning cycles (before cycling at 0.5 C rate) and (b) after 200 cycles at 25 °C.

component to reflect the depressed semicircular shape. Before cycling (after two preconditioning cycles), the electrolyte resistance and interfacial resistances (*i.e.*, sum of R_f and R_{ct}) were lowest in the cell that employed the liquid electrolyte with the fibrous PAN membrane. This result indicates that a cross-linking reaction inevitably retards not only ion transport in the polymer electrolyte but also charge transfer at the electrolyte-electrode interface. After 200 cycles, interfacial resistance increased for all cells. An increase in interfacial resistance is related to both growth of the resistive surface layer on the electrodes and deterioration of the interfacial contacts at electrodes. Unlike the AC impedance data shown in Fig. 8(a), the cell with the PAN(SiO₂)-based cross-linked composite polymer electrolyte had the lowest interfacial resistance after repeated cycling. The cross-linked composite polymer layer containing SiO₂ particles effectively trapped the electrolyte solution and reduced the harmful reactions between organic solvents and electrodes. This feature ultimately limited the growth of the resistive layer on electrode surfaces and enhanced the interfacial stability. This result is consistent with those of previous studies which showed that the addition of an inorganic filler was effective at stabilizing the electrode interfacial resistance.^{35,36} Chemical cross-linking in the presence of reactive SiO₂ particles also helped to intimately adhere the PAN membrane to electrodes, providing favorable interfacial charge transport between the electrolyte and electrodes during cycling.

After cycling, the electrolyte resistance was highest in the cell that employed the liquid electrolyte with the fibrous PAN membrane. This result is ascribed to the loss of the electrolyte solution due to leakage as well as deleterious reactions between the organic solvents and electrodes. These results imply that *in situ* cross-linking of the electrolyte solution in the presence of vinyl-functionalized SiO₂ particles was effective for maintaining the interfacial contact between the electrodes and the electrolyte, as well as holding the electrolyte solution in the cell. As a result, the cell with the cross-linked composite polymer electrolyte exhibited the most stable cycling performance, as shown in Fig. 7(b).

Fig. 9 compares the discharge capacities of lithium-ion polymer cells assembled with different polymer electrolytes during experiments in which the C rate increased gradually every five cycles within the range of 0.2 to 2.0 C. The discharge capacities gradually decreased as the C rate increased, thereby demonstrating polarization. The discharge capacities of the cell that employed the liquid electrolyte with the fibrous PAN membrane were higher than those of cells with cross-linked polymer electrolytes. The ionic resistance was lowest in the cell that employed the liquid electrolyte with the fibrous PAN membrane, thereby reducing the concentration polarization of the electrolyte during cycling. Comparison of the rate capabilities of the two cells with cross-linked polymer electrolytes showed that the use of reactive SiO₂ particles improved the high rate performance. This result is ascribed to the favorable interfacial charge transport between the electrodes and electrolyte in the cell, as shown in Fig. 8.

To evaluate the high-temperature cycling stability of cells, a cycling test was performed at 55 °C. Fig. 10(a) shows the discharge capacities of lithium-ion polymer cells assembled with different polymer electrolytes as a function of cycle number, obtained at 55 °C and 0.5 C rate. The cells delivered initial discharge capacities ranging from 208.6 to 210.5 mA h g⁻¹, slightly higher than those obtained at 25 °C. Note that a cell assembled with the fibrous PAN membrane and liquid electrolyte showed drastic capacity fading to 117.1 mA h g⁻¹ after 200 cycles, which is only about 55.6% of the initial discharge capacity. Among all cells, the cell with the PAN(SiO₂)-based

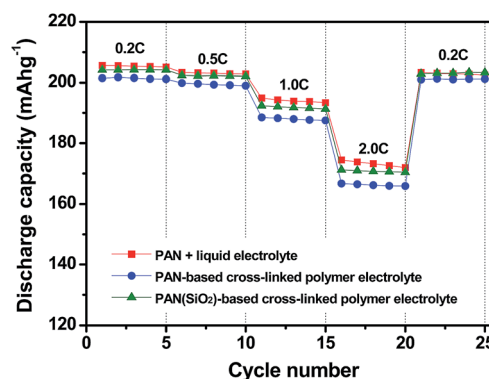


Fig. 9 Discharge capacities of lithium-ion polymer cells assembled with different polymer electrolytes as a function of C rate.

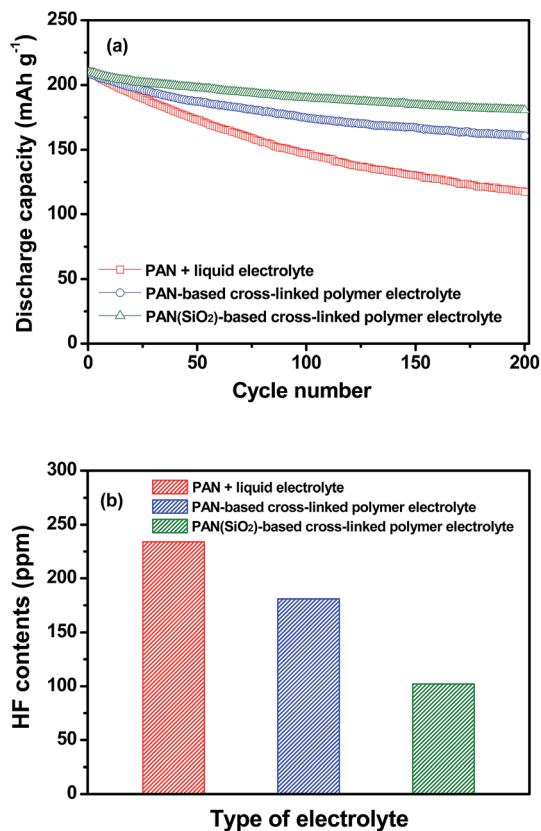


Fig. 10 (a) Discharge capacities of lithium-ion polymer cells assembled with different polymer electrolytes at 55 °C (0.5 C CC and CV charge, 0.5 C CC discharge, cut-off voltage: 2.6–4.3 V), and (b) HF contents in different types of electrolytes after storage at 55 °C for 1 week.

cross-linked composite polymer electrolyte exhibited the best cycling stability at 55 °C. Layered cathode active materials experience gradual capacity fading at high temperatures due to structural and interfacial instabilities as well as dissolution of transition metals from the active cathode material by HF attack.^{37,38} According to previous studies, HF is generated by thermal decomposition and hydrolysis of LiPF₆ due to the trace moisture in the electrolyte solution.^{39,40} In cells with PAN or PAN(SiO₂)-based cross-linked polymer electrolyte, the cross-linked polymer network formed on the electrode surface protects the active LiNi_{0.8}Co_{0.15}Al_{0.05}O₂ material from HF attack. In addition, the SiO₂ particles in the cross-linked composite polymer electrolyte play the role of HF scavengers³⁹ in reducing the HF content in the electrolyte, as presented in Fig. 10(b). Accordingly, the use of the cross-linked composite polymer electrolyte containing SiO₂ particles reduced the HF content and suppressed the dissolution of transition metals from the active cathode material at elevated temperatures. As a result, the cell assembled with the PAN(SiO₂)-based cross-linked composite polymer electrolyte exhibited the most stable cycling behavior at 55 °C. In the cell employing the liquid electrolyte with the fibrous PAN membrane, the dissolution of transition metals by HF attack possibly caused a rapid increase in the interfacial resistance, thereby accelerating the capacity loss as cycling

progressed at elevated temperatures. These results imply that *in situ* cross-linking of the electrolyte in the presence of reactive SiO₂ particles on the fibrous PAN membrane achieves superior capacity retention at high temperatures.

Conclusions

Vinyl-functionalized SiO₂ nanoparticles were synthesized for use as cross-linking sites as well as inorganic filler in the preparation of a composite polymer electrolyte. The cross-linked composite polymer electrolyte was prepared by the *in situ* cross-linking reaction using a fibrous PAN membrane, reactive SiO₂ particles and electrolyte solution containing a small amount of TEGDA. The composite polymer electrolyte encapsulated the electrolyte solution without solvent leakage and exhibited enhanced thermal stability. *In situ* cross-linking in the presence of vinyl-functionalized SiO₂ particles also promoted strong interfacial adhesion between electrodes and the electrolyte, resulting in low interfacial resistances during cycling. Consequently, the cell assembled with the cross-linked composite polymer electrolyte using the fibrous PAN membrane and vinyl-functionalized SiO₂ particles exhibited high discharge capacity and good cycling stability.

Acknowledgements

This work was supported by the National Research Foundation of Korea Grant funded by the Korean government (MEST) (NRF-2009-C1AAA001-0093307) and the R&D Convergence Program of NST (National Research Council of Science & Technology) of Republic of Korea.

References

- 1 K. Xu, *Chem. Rev.*, 2004, **104**, 4303.
- 2 M. Armand, F. Endres, D. R. MacFarlane, H. Ohno and B. Scrosati, *Nat. Mater.*, 2009, **8**, 621.
- 3 R. Marom, S. F. Amalraj, N. Leifer, D. Jacob and D. Aurbach, *J. Mater. Chem.*, 2011, **21**, 9938.
- 4 E. Quartarone and P. Mustarelli, *Chem. Soc. Rev.*, 2011, **40**, 2525.
- 5 K. Xu, *Chem. Rev.*, 2014, **114**, 11503.
- 6 J. Y. Song, Y. Y. Wang and C. C. Wan, *J. Power Sources*, 1999, **77**, 183.
- 7 J. Hassoun, P. Reale and B. Scrosati, *J. Mater. Chem.*, 2007, **17**, 3668.
- 8 J. W. Fergus, *J. Power Sources*, 2010, **195**, 4554.
- 9 K. Murata, S. Izuchi and Y. Yoshihisa, *Electrochim. Acta*, 2000, **45**, 1501.
- 10 Z. Wen, T. Itoh, T. Uno, M. Kubo and O. Yamamoto, *Solid State Ionics*, 2003, **160**, 141.
- 11 J. A. Choi, Y. Kang, H. Shim, D. W. Kim, H. K. Song and D. W. Kim, *J. Power Sources*, 2009, **189**, 809.
- 12 J. Reiter, R. Dominko, M. Nadherná and I. Jakubec, *J. Power Sources*, 2009, **189**, 133.
- 13 J. A. Choi, Y. Kang, H. J. Shim, D. W. Kim, E. H. Cha and D. W. Kim, *J. Power Sources*, 2010, **195**, 6177.

- 14 M. Patel and A. J. Bhattacharyya, *Energy Environ. Sci.*, 2011, **4**, 429.
- 15 Y. W. Lee, W. K. Shin and D. W. Kim, *Solid State Ionics*, 2014, **255**, 6.
- 16 D. Zhou, Y.-B. He, Q. Cai, X. Qin, B. Li, H. Du, Q.-H. Yang and F. Kang, *J. Mater. Chem. A*, 2014, **2**, 20059.
- 17 J. Fan and P. S. Fedkiw, *J. Electrochem. Soc.*, 1997, **144**, 399.
- 18 F. Croce, G. B. Appetecchi, L. Persi and B. Scrosati, *Nature*, 1998, **394**, 456.
- 19 N. Byrne, J. Efthimiadis, D. R. MacFarlane and M. Forsyth, *J. Mater. Chem.*, 2004, **14**, 127.
- 20 H. Han, W. Liu, J. Zhang and X.-Z. Zhao, *Adv. Funct. Mater.*, 2005, **15**, 1940.
- 21 A. S. Arico, P. Bruce, B. Scrosati, J.-M. Tarascon and W. Van Schalkwijk, *Nat. Mater.*, 2005, **4**, 366.
- 22 S. K. Das, S. S. Mandal and A. J. Bhattacharyya, *Energy Environ. Sci.*, 2011, **4**, 1391.
- 23 Z. Jia, W. Yuan, H. Zhao, H. Hu and G. L. Baker, *RSC Adv.*, 2014, **4**, 41087.
- 24 Y. S. Lee, S. H. Ju, J. H. Kim, S. S. Hwang, J. M. Choi, Y. K. Sun, H. Kim, B. Scrosati and D. W. Kim, *Electrochem. Commun.*, 2012, **17**, 18.
- 25 S. H. Ju, Y. S. Lee, Y. K. Sun and D. W. Kim, *J. Mater. Chem. A*, 2013, **1**, 395.
- 26 Y. S. Lee, J. H. Lee, J. A. Choi, W. Y. Yoon and D. W. Kim, *Adv. Funct. Mater.*, 2013, **23**, 1019.
- 27 W. K. Shin, Y. S. Lee and D. W. Kim, *J. Mater. Chem. A*, 2014, **2**, 6863.
- 28 J. Zhao, S. G. Jo and D. W. Kim, *Electrochim. Acta*, 2014, **142**, 261.
- 29 J. P. Blitz, R. S. S. Murthy and D. E. Leyden, *J. Colloid Interface Sci.*, 1988, **121**, 63.
- 30 P. Siberzan, L. Leger, D. Ausserre and J. J. Benatta, *Langmuir*, 1991, **7**, 1647.
- 31 D. Zhang, A. B. Karki, D. Rutman, D. P. Young, A. Wang, D. Cockea, T. H. Ho and Z. Guo, *Polymer*, 2009, **50**, 4189.
- 32 M. D. Levi, G. Salitra, B. Markovsky, H. Teller, D. Aurbach, U. Heider and L. Heider, *J. Electrochem. Soc.*, 1999, **146**, 1279.
- 33 Y. Bai, X. Wang, X. Zhang, H. Shu, X. Yang, B. Hu, Q. Wei, H. Wu and Y. Song, *Electrochim. Acta*, 2013, **109**, 355.
- 34 T. Liu, A. Garsuch, F. Chesneau and B. L. Lucht, *J. Power Sources*, 2014, **269**, 920.
- 35 C. M. Yang, H. S. Kim, B. K. Na, K. S. Kum and B. W. Cho, *J. Power Sources*, 2006, **156**, 574.
- 36 S. J. Lim, Y. S. Kang and D. W. Kim, *Electrochim. Acta*, 2011, **56**, 2031.
- 37 G. G. Amatucci, J. M. Tarascon and L. C. Klein, *Solid State Ionics*, 1996, **83**, 167.
- 38 S. U. Woo, B. C. Park, C. S. Yoon, S. T. Myung, J. Prakash and Y. K. Sun, *J. Electrochem. Soc.*, 2007, **154**, A649.
- 39 S. F. Lux, I. T. Lucas, E. Pollak, S. Passerini, M. Winter and R. Kostecki, *Electrochem. Commun.*, 2012, **14**, 47.
- 40 Y. Okamoto, *J. Electrochem. Soc.*, 2013, **160**, A404.